Radiotherapy and Oncology 114 (2015) 206–211

Contents lists available at ScienceDirect

Radiotherapy and Oncology

journal homepage: www.thegreenjournal.com

Normal tissue doses in Hodgkin lymphoma

A new method to estimate doses to the normal tissues after past extended and involved field radiotherapy for Hodgkin lymphoma

Maja V. Maraldo [a,*], Michael Lundemann [a], Ivan R. Vogelius [a], Lena Specht [a,b]

[a] Department of Oncology, Section of Radiotherapy; and [b] Department of Hematology, Rigshospitalet, University of Copenhagen, Denmark

ARTICLE INFO

Article history:
Received 8 September 2014
Received in revised form 9 January 2015
Accepted 9 January 2015
Available online 22 January 2015

Keywords:
Dose estimates
Hodgkin lymphoma
Extended field
Involved field
Normal tissues

ABSTRACT

Introduction: Reconstruction of radiotherapy (RT) performed decades ago is challenging, but is necessary to address dose–response questions from epidemiological data and may be relevant in re-irradiation scenarios. Here, a novel method to reconstruct extended and involved field RT for patients with Hodgkin lymphoma was used.

Materials and methods: For 46 model patients, 29 organs at risk (OARs) were contoured and seven treatment fields reconstructed (mantle, mediastinal, right/left neck, right/left axillary, and spleen field). Extended and involved field RT were simulated by generating RT plans by superpositions of the seven individual fields. The mean (standard deviation) of the 46 individual mean organ doses were extracted as percent of prescribed dose for each field superposition.

Results: The estimated mean doses to the OARs from 17 field combinations were presented. The inter-patient variability was found to be a larger contributor to the uncertainty than the field simulation process. The inter-patient variability depended on the OAR and primarily affected the estimates for OARs located at the edge of the RT field.

Conclusions: Dose estimates for 29 OARs were reported from extended and involved field RT. These estimates could be employed when individual reconstruction is not feasible and estimated doses from past treatments are needed.

 Radiotherapy and Oncology 114 (2015) 206–211

The treatment of Hodgkin lymphoma (HL) has changed considerably over the last decades, from extended field radiotherapy (RT) as the sole treatment to combined modality treatment, with combination chemotherapy followed by consolidation RT [1–3]. Due to the increased efficacy of combination chemotherapy and technological advances, both the radiation dose and the size of the RT fields have been reduced [3–6].

A large group of HL survivors exists treated with now outdated treatment regimens including extensive RT fields to high doses. These survivors are at risk of not only relapsed disease, but also treatment-induced late effects such as cardiovascular disease and secondary cancers [7,8]. A detailed knowledge of the individual exposure may help to identify patients in need of more intense monitoring as well as aid in the interpretation of complaints and clinical findings during follow-up. Accordingly, a 3D reconstruction of radiation dose delivered to patients treated with past techniques remains important. In clinical practice it is, however, challenging to reconstruct individual treatment plans, especially if planned with 2D technique and delivered with anteroposterior-posteroanterior (APPA) fields up to several decades ago, as treatment records may be missing and the only available information is the patient's recollection of the prescribed dose and field location.

Here, we use a novel method to estimate radiation doses to the organs at risk (OARs) in the thorax, and the head and neck regions from extended field RT and different combinations of involved field RT that were commonly used from the 1960s to the mid-2000s. Data on treatment-induced late effects arise from patients treated during this time period, primarily through observational studies with limited information on individual treatment exposure [7,9,10,8]. The risk of late effects can be used in combination with these dose estimates for dose–response analyses as well as to quantify the risk reduction obtained with modern treatment. Also, for individual patients it could allow for more precise estimates of the past organ exposure.

Abbreviations: LMCA, left main coronary artery; LADCA, left anterior descending coronary artery; LCCA, left circumflex coronary artery; RCA, right coronary artery; CCA, common carotid artery; ECA, external carotid artery; ICA, internal carotid artery; parotid, parotid gland; submand, submandibular gland.

* Corresponding author at: Department of Oncology, Section of Radiotherapy, Rigshospitalet, Blegdamsvej 9, DK-2100 Copenhagen, Denmark.
E-mail address: dra.maraldo@gmail.com (M.V. Maraldo).

http://dx.doi.org/10.1016/j.radonc.2015.01.008
0167-8140/

Methods

The method is based on virtual simulation and computed tomography (CT)-based treatment planning to reconstruct multiple past RT fields on a cohort of patients with early stage HL.

Model patients

All patients with early stage, classical HL treated with RT at our institution from 2006–2010 were considered for the study. Forty-six patients had CT scans suitable for the reconstruction of a mantle field (MF), i.e., the patient was scanned from the base of scull to at least the 11th thoracic vertebra. We use these 46 consecutively treated patients as model patients, 25 were male, 21 female and the median age at diagnosis was 34 years (range: 15–76 years).

Contouring of organs at risk

Relevant OARs were contoured on the planning CT scans of the 46 model patients. In the thorax, the heart, the coronary arteries, the heart valves, the lungs, the female breasts, and the esophagus were contoured as specified in [11–13]. In the head and neck region, the thyroid gland, neck muscles, pharynx, larynx and the right and left parotid and submandibular glands, as well as the right and left common carotid arteries, external carotid arteries and internal carotid arteries were contoured as described previously [14,15]. In the abdomen, the stomach and spleen were contoured for the 21 patients for whom the CT scan included the entirety of these organs (hereafter referred to as spleen patients). The contouring was done retrospectively by a radiation oncologist (MM). All CT scans were performed with contrast and a slice thickness of 2.5 mm (22 patients) or 3.0 mm (24 patients).

Reconstruction of radiotherapy fields

Historically, the lymph node regions defined by the Ann Arbor staging classification [16] were used to define the borders of the RT fields for both extended and involved field RT. Extended field RT was delivered as a MF supradiaphragmatically plus the paraaortic lymph nodes and spleen in sub-total nodal irradiation. Total nodal irradiation additionally included the iliac and inguinal lymph node regions. For involved field RT, The European Organisation for Research and Treatment of Cancer (EORTC) H9 trial [17,18] protocol was used to define the borders of the different fields: a right and left neck field (supraclavicular and cervical lymph node region), a right and left axillary field (infraclavicular and axillary region), and a mediastinal field (mediastinum including the hilar nodes). A spleen field was also constructed. The individual fields were simulated on the planning CT scan using bony landmarks on the digitally reconstructed radiograph to mimic 2D planning.

Six supradiaphragmatic treatment plans (right/left neck, right/left axilla, mediastinum, MF), were generated for each of the 46 model patients in Eclipse (version 10, Varian Medical Systems) with APPA fields, using 6 MV photon beams, a collimator angle of 45° and a skin-source distance of 100 cm. Additionally, spleen fields were set up for the 21 spleen patients. All field doses were calculated as a two-step process. First, the plan calculation was made without heterogeneity correction. Thereafter, the heterogeneity correction was enabled and dose was recalculated with the same number of monitor units as in step I in order to mimic the historical prescription process, but using modern dose calculation to assess the actual dose deposition. All dose calculations were done with the AAA algorithm [19]. The prescribed dose to each field was set to 30 Gy in 2 Gy fractions, 5 fractions per week.

Radiotherapy plan simulations

A total of 31 possible combinations of fields existed for extended and involved field RT where one or more lymph node regions were involved. Fifteen field combinations which were used for less than 1% of the irradiated patients in the EORTC H9 trial were not considered further. Dose estimates for combinations with additional spleen irradiation were limited to the MF because spleen irradiation was abandoned with the introduction of involved field RT. The estimated doses for the MF with spleen irradiation were based on the 21 spleen patients, and estimated doses to the right and left breast were based on the 21 female patients. RT plans with the 17 field combinations were simulated from superposition of the seven individual plans as illustrated in Fig. 1. The final dose in each voxel was determined by the maximum dose in the corresponding voxels of the individual fields. All plan simulations were performed in MATLAB (The MathWorks, Natick, MA) using in-house routines in combination with the CERR toolbox [20]. Simulations were done with and without a spleen field for combinations which included a mediastinal field. The mean of the 46 individual mean doses to the 29 OARs was extracted as percent (%) of prescribed dose. Mean dose estimates from a full MF versus a MF simulated from five individual fields were compared in order to evaluate the accuracy of the field superposition. The inter-patient variability, i.e., the range in dose estimates from the 46 model patients, was calculated for each of the different OARs.

The patient characteristics of the 46 model patients, the definition of the individual RT field borders, number of irradiated patients for each field combination in the H9 trial, full table of results, the inter-patient variability with all field combinations, mean OAR DVHs for each field combination, and Matlab scripts are provided as Supplementary material.

Results

In Table 1, the estimated mean doses to the OARs in the thorax and abdomen as well as the 17 different field combinations are presented. From Table 1 it is seen how the estimated mean doses to the heart and the cardiac substructures (i.e., the coronary arteries and heart valves) are identical whenever the combination of RT fields includes a mediastinal field, irrespective of further additional fields. Also, when the plan includes a spleen field the mean dose estimates to the heart, the left anterior descending coronary artery, the lungs and the left female breast are increased by 20%, 29%, 15%, and 31%, respectively. However, the mean dose estimates to the remaining thoracic structures are less affected. With spleen irradiation, the mean dose estimates to the spleen and stomach are increased dramatically to 98% (±12%) and 76% (±18%) of prescribed dose irrespective of field combinations. For involved field RT, the mean dose to the right and left female breast is 15% and 16%, respectively, with a mediastinal field or with a mediastinal and right and/or left neck field. However, the mean breast dose is increased by 169% when an axillary field is added in the corresponding side. The mean dose estimates for the thoracic organs are limited to the leakage dose for involved field plans including only neck or axillary fields, except for the lungs which receive 13% (±2%) of prescribed dose from an axillary field.

The estimated mean doses to the head and neck OARs for the 17 field combinations are presented in Table 2. All OARs are estimated to receive a high dose with MF irradiation and the mean dose estimates are unchanged by the inclusion of a spleen field. Also, the laterality of the field becomes important with involved field RT. The estimated dose is equivalent to that of a MF if the OARs are included in the RT field whereas it is reduced to only the leakage dose for the remaining organs.

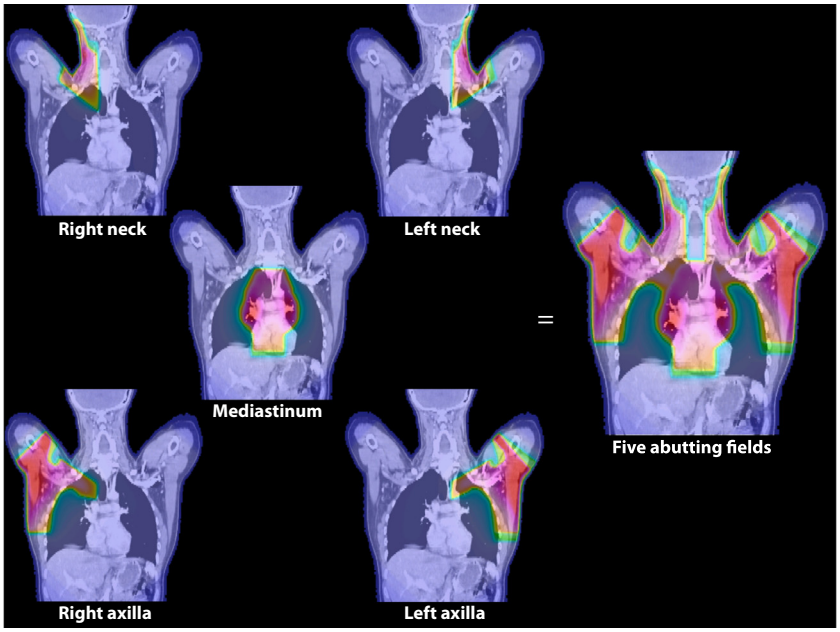

Fig. 1. Illustration of the field superposition process. A mantle field is simulated from five individual fields. The resulting plan is created by choosing the maximum dose contribution in each volume element (voxel) from each of the five abutting fields.

Table 1
Mean dose estimates for organs at risk in the thorax and abdomen with the 17 most common combinations of radiotherapy fields in% of prescribed dose.

Most common combinations	Heart	LMCA	LAD	LCCA	RCA	Aortic valve	Pulmonic valve	Mitral valve	Tricuspid valve	Lungs	Right female breast	Left female breast	Esophagus	Spleen	Stomach
Mantle field	65.1	91.9	56.2	88.7	91.4	90.6	94.8	81.3	82.6	45.2	39.6	43.2	75.0	5.7	8.1
Mantle field and spleen irradiation	77.8	92.9	72.5	94.1	93.6	92.4	95.7	86.8	86.9	52.1	43.9	56.5	77.6	97.9	75.7
Mediastinum	65.1	91.9	56.2	88.7	91.4	90.6	94.8	81.3	82.6	39.0	14.5	16.3	74.9	5.7	8.1
Mediastinum, NeckR	65.1	91.9	56.2	88.7	91.4	90.6	94.8	81.3	82.6	39.0	14.5	16.3	74.9	5.7	8.1
Mediastinum, NeckL	65.1	91.9	56.2	88.7	91.4	90.6	94.8	81.3	82.6	39.0	14.5	16.3	74.9	5.7	8.1
Mediastinum, NeckR, NeckL	65.1	91.9	56.2	88.7	91.4	90.6	94.8	81.3	82.6	39.0	14.5	16.3	74.9	5.7	8.1
Mediastinum, NeckR, NeckL, AxillaR	65.1	91.9	56.2	88.7	91.4	90.6	94.8	81.3	82.6	39.0	14.5	16.3	74.9	5.7	8.1
Mediastinum, NeckR, NeckL, AxillaL	65.1	91.9	56.2	88.7	91.4	90.6	94.8	81.3	82.6	39.0	14.5	16.3	74.9	5.7	8.1
Mediastinum, NeckR, AxillaR	65.1	91.9	56.2	88.7	91.4	90.6	94.8	81.3	82.6	39.0	14.5	16.3	74.9	5.7	8.1
Mediastinum, NeckL, AxillaL	65.1	91.9	56.2	88.7	91.4	90.6	94.8	81.3	82.6	39.0	14.5	16.3	74.9	5.7	8.1
NeckR	4.6	4.8	4.6	5.0	4.6	4.6	4.7	4.6	4.4	7.4	4.8	4.5	6.1	3.6	4.1
NeckL	4.6	4.9	4.8	5.2	4.5	4.6	4.9	4.7	4.4	7.3	4.5	4.7	7.6	3.7	4.2
NeckR, NeckL	4.8	5.0	4.9	5.3	4.7	4.8	5.0	4.7	4.6	9.5	4.8	4.8	8.0	3.7	4.3
NeckR, AxillaR	5.6	5.8	5.4	5.7	5.9	5.8	5.7	5.4	5.5	13.3	32.2	5.1	7.2	3.8	4.5
NeckL, AxillaL	5.8	6.4	6.4	7.2	5.5	5.8	6.6	5.8	5.3	12.8	5.1	34.0	9.0	4.6	5.1
AxillaR	5.6	5.8	5.4	5.7	5.9	5.8	5.7	5.4	5.5	13.0	32.2	5.1	6.9	3.8	4.5
AxillaL	5.8	6.4	6.4	7.2	5.5	5.8	6.6	5.8	5.3	12.6	5.1	34.0	8.1	4.5	5.1

Abbreviations: LMCA – left main coronary artery, LAD – left anterior descending coronary artery, LCCA – left circumflex coronary artery, RCA – right coronary artery, NeckR – right neck region, NeckL – left neck region, AxillaR – right axillary region, AxillaL – left axillary region.
Results are presented as the mean of the 46 model patients (for full table of results see Supplementary material).
Most common combinations defined as the field combinations registered for 1% or more of patients in the EORTC H9 trial.

Table 2
Mean dose estimates for organs at risk in the head and neck region with the 17 most common combinations of radiotherapy fields in % of prescribed dose.

Most common combinations	Parotid gland		Submandibular gland		Thyroid gland	Neck muscles	Pharynx	Larynx	Common carotid artery		External carotid artery		Internal carotid artery	
	Right	Left	Right	Left					Right	Left	Right	Left	Right	Left
Mantle field	79.2	78.2	67.7	63.1	42.1	73.6	14.3	11.4	88.6	80.1	57.0	54.1	49.0	47.2
Mantle field and spleen irradiation	79.2	78.2	67.7	63.1	42.1	73.6	14.3	11.4	88.6	80.1	57.0	54.1	49.0	47.2
Mediastinum	5.8	5.9	6.3	6.3	20.9	7.5	5.9	7.6	64.0	50.4	5.9	5.9	5.8	5.8
Mediastinum, NeckR	79.2	6.0	67.7	6.4	34.2	40.9	11.1	10.3	88.6	50.4	57.0	6.2	49.0	6.1
Mediastinum, NeckL	5.9	78.3	6.6	63.0	28.9	39.8	9.8	9.2	64.0	80.2	6.1	54.1	6.0	47.1
Mediastinum, NeckR, NeckL	79.2	78.2	67.7	63.1	42.1	72.8	14.2	11.4	88.6	80.1	57.0	54.1	49.0	47.2
Mediastinum, NeckR, NeckL, AxillaR	79.2	78.2	67.7	63.1	42.1	73.2	14.3	11.4	88.6	80.1	57.0	54.1	49.0	47.2
Mediastinum, NeckR, NeckL, AxillaL	79.2	78.2	67.7	63.1	42.1	73.2	14.2	11.4	88.6	80.1	57.0	54.1	49.0	47.2
Mediastinum, NeckR, AxillaR	79.2	6.1	67.4	6.6	34.2	41.2	11.1	10.3	88.6	50.5	57.0	6.3	49.0	6.2
Mediastinum, NeckL, AxillaL	6.8	78.3	6.6	63.0	28.9	40.2	9.8	9.2	64.0	80.2	6.1	54.1	6.0	47.1
NeckR	79.2	5.4	67.4	5.9	23.5	40.2	11.0	10.0	43.2	6.7	57.0	6.0	49.0	5.9
NeckL	5.4	78.3	6.0	63.0	17.3	39.2	9.8	8.8	7.0	54.7	5.9	54.1	5.8	47.1
NeckR, NeckL	79.2	78.2	67.7	63.1	33.7	72.8	14.2	11.2	43.6	54.7	57.0	54.1	49.0	47.1
NeckR, AxillaR	79.2	5.8	67.4	6.2	23.6	40.7	11.1	10.0	45.2	7.4	57.0	6.2	49.0	6.1
NeckL, AxillaL	5.5	78.3	6.1	63.0	17.4	39.6	9.8	8.8	7.6	57.6	5.9	54.1	5.8	47.1
AxillaR	6.5	5.7	6.4	5.8	7.5	9.0	5.7	6.6	14.8	7.1	6.2	5.7	6.1	5.8
AxillaL	5.5	6.5	5.6	6.3	7.3	9.1	5.6	6.5	7.4	18.8	5.5	6.1	5.4	5.9

Abbreviations: NeckR – right neck region, NeckL – left neck region, AxillaR – right axillary region, AxillaL – left axillary region.
Results are presented as the mean of the 46 model patients (for full table of results see Supplementary material).
Most common combinations defined as the field combinations registered for 1% or more of patients in the EORTC H9 trial.

In Fig. 2, the simulation error for the mean dose estimates from a full MF versus a MF simulated from 5 individual fields are illustrated for the lungs (large organ), the esophagus (long organ) and the thyroid gland (organ at the edge of the field). The mean dose estimates for the lungs are aligned close to the identity line, indicating a high accordance between the full MF and the simulated MF, whereas mean dose estimates for the thyroid gland are not. Also, the dispersion of mean dose estimates for the 46 model patients, illustrated by the gray bar, is very different for the lungs, the esophagus and the thyroid gland. This inter-patient variability is a much larger contributor to the uncertainty in the mean dose estimates than the field simulation process. Fig. 3 illustrates how the simulated MF differs from a full MF as some structures in the neck, such as the thyroid gland and the larynx, are not included in the field due to the sparing of the spinal cord in the individual cervical fields. As the cervical fields are superposed the midline structures will appear under-dosed when compared to a full MF.

The standard deviation in mean dose estimates from a simulated MF for the 46 model patients are plotted against the mean estimated mean dose for each of the 29 OARs in Fig. 4. For the OARs plotted to the left, the inter-patient variability is low whereas the variability is higher the more to the right the individual organ is plotted. The variability especially affects the OARs located close to the edge of the field, such as the thyroid gland, the submandibular glands and the mitral and tricuspid valves (cf. Fig. 3).

Discussion

Here, we present a method which allows for an estimation of the mean dose to 29 different OARs in the head and neck, thorax, and abdomen with 17 possible combinations of extended and involved field radiotherapy for early stage HL, provided the dose and field type is known.

Strong features of our study are the number of model patients, the individual contouring, and the field superposition process. By using a large number of model patients it is possible to demonstrate the existence of a substantial inter-patient variability. The effect of the inter-patient variability should not be underestimated, especially with smaller RT fields: with large fields the OARs are included in their entirety but as the field is diminished only part of the organ is irradiated and the dose estimates will vary more between patients than had the organ been fully included within the field. Therefore, the inter-patient variability in estimated dose to a specific OAR will differ with each of the 17 possible field combinations (see Supplementary material). Our findings highlight the importance of an adequate number of model patients for retrospective dose reconstruction in order to capture the variation within the population of interest, especially in studies which wish to correlate treatment exposure to the risk of the late effects. Although individual re-planning should always be encouraged, it is impossible in follow-up studies with very large patient cohorts. Different approaches have been employed to overcome this obstacle, either by an estimate of dose from individual treatment records applied to a "representative" patient [21,22] or a water phantom [23–25], or by only reporting the prescribed dose to the different field types [7,9]. Our method allows for a "group" estimate, including young and old as well as male and female patients which provides an interval within which the delivered dose is likely to lie. Thus, our estimates could help provide 3D dose information for patients from large, historical cohorts for dose–response analyses. Admittedly, such extrapolations would be associated with uncertainties. However, approximations are inherent to the discipline of retrospective dosimetry and cannot be avoided. Even individual re-planning has its own problems: The largest variability in this study was seen at the edge of the treatment fields, and so, a detailed knowledge of past fields and field borders is needed when doing re-planning. Also, the absence of CT scans for historical patients and the absence of daily image guidance even in modern series will limit the precision of some OAR dose estimates despite individual estimates.

We have chosen to simulate RT plans on 3D planning CT scans of contemporary patients, and fields are reconstructed regardless of actual involvement with strict adherence to the field definitions and without consideration of clinical parameters such as prior

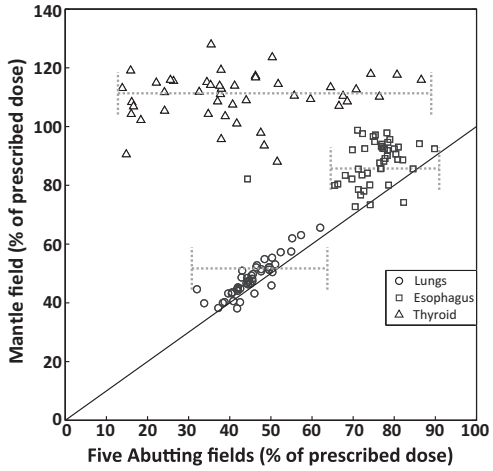

Fig. 2. Scatterplot of mean dose estimates for a mantle field versus a mantle field simulated from five abutting fields. Mean dose estimates for a mantle field versus a simulated mantle field from five abutting fields in percent of prescribed dose are plotted for the lungs (circles), the esophagus (squares) and the thyroid (triangles) for the 46 model patients. The full, black line is the identity line and the gray, dotted bars illustrate the range in estimates between patients for the three organs (excluding an outlier for the esophagus).

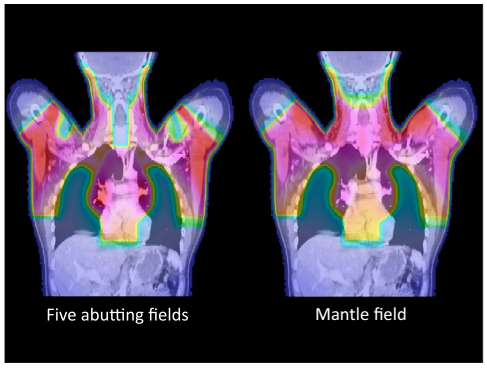

Fig. 3. The mantle field simulated from five abutting fields compared to a full mantle field. The five abutting fields are seen to under-dose structures in the midline of the neck, compared to the mantle field, due to the individual cervical fields which are set to spare the spinal cord.

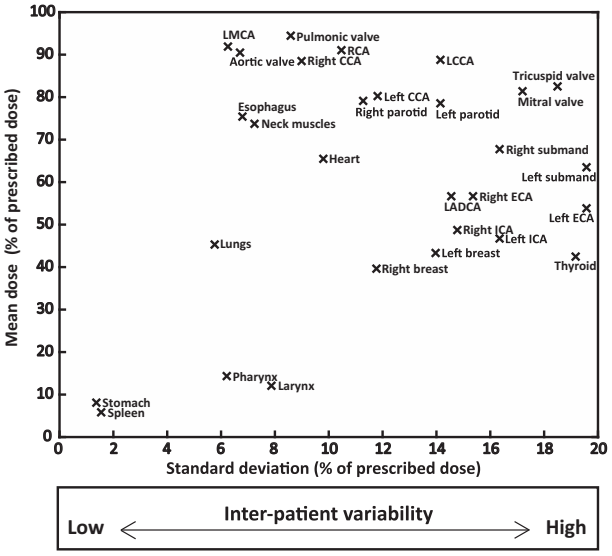

Fig. 4. Inter-patient variability in mean dose estimates for the organs at risk for a simulated mantle field. The standard deviation (in percent of prescribed dose) in mean dose estimates with a simulated mantle field for the 46 model patients are plotted against the mean of the mean dose estimate (in percent of prescribed dose) for the 29 different organs at risk. The higher the standard deviation in mean dose estimates, the higher the inter-patient variability.

chemotherapy or co-morbidities. Although assumptions must be made to reconstruct a 2D planning situation to modern 3D treatment planning systems, the method provides 3D planning data. All plans are calculated using 2 Gy fractions, irrespective of the actual treatment given to the individual model patient, and the dose estimates are reported in percent of prescribed dose. This facilitates that dose estimates can be recalculated for patients treated with other dose schedules. Also, rather than reconstructing 17 individual plans for each model patient, the possible field combinations are obtained by superposing only seven individual plans. The automatic simulation process thus ensures that field volumes and borders are congruous for the individual model patient with each of the involved field combinations.

Others have tried to estimate the delivered dose from past RT regimens [12–15,26–28], however, only in the form of extended field RT. The majority of these studies performs an individualized field simulation for contemporary patients in order to quantify the reduction in radiation exposure, and thereby the reduced risk of late effects, obtained with current regimens from a reduction in field size and/or prescribed dose. Our method has a reversed approach in that we wish to estimate the exposure for patients treated in the past, not only with extended but also with involved field RT. This allows for a clinical use as individual reconstruction of prior treatment requires special knowledge. In the situation where little information is available, the dose estimates presented here should be a fairly reasonable approximation for the majority of HL survivors, provided information on field type and prescribed dose can be recovered or estimated.

Another application of our results could be to correlate the dose estimates to the reported risks of late effects from past patients in a more detailed manner in order to quantify the risk reduction obtained with current regimens. Treatment exposure in many observational studies are often limited to a dichotomous yes/no or more or less than 30 Gy prescribed dose [7,9,10] which reduces the utility of results, especially after the introduction of more conformal target definitions [29]. When only the prescribed dose is noted in the literature, the dose estimates presented here can serve as an indication of the organ exposure. However, it should be emphasized that our RT reconstruction does not reflect all the heterogeneity with which RT has been delivered in the past, especially with regard to the use of different energy photons (e.g., Cobalt machines), anterior, lateral or dorsal beam entry techniques, and the use of cardiac blocking. Furthermore, historical treatments may have been delivered with now substandard quality assurance or techniques, such as alternating fields on alternating days, which are now known to be inappropriate. Using our data for scientific analyses should, therefore, be undertaken with the appropriate consideration of the underlying assumptions and insufficiencies.

In conclusion, 17 possible combinations of extended and involved field RT plans are reconstructed for early stage Hodgkin lymphoma and the radiation doses to 29 different organs at risk in the thorax, and the head and neck regions are estimated. These estimates may be employed in clinical and research situations where knowledge of radiation doses to normal structures from past treatments is needed.

Conflicts of interest

The authors declare no conflicts of interests.

Funding

The work herein was supported by a Grant from Rigshospitalet Scientific Research Committee, Copenhagen, Denmark.

Acknowledgements

We thank Francesco Giusti, PhD, Catherine Fortpied, MSc, and Safaa Ramadan, MD, PhD at the EORTC headquarters in Belgium for their help with data extraction; the EORTC lymphoma group is greatly acknowledged for their permission to use data from the EORTC-GELA H9 trial.

Appendix A. Supplementary data

Supplementary data associated with this article can be found, in the online version, at http://dx.doi.org/10.1016/j.radonc.2015.01.008.

References

[1] Eich HT, Diehl V, Gorgen H, et al. Intensified chemotherapy and dose-reduced involved-field radiotherapy in patients with early unfavorable Hodgkin's lymphoma: final analysis of the German Hodgkin Study Group HD11 trial. J Clin Oncol 2010;28:4199–206.
[2] Engert A, Plutschow A, Eich HT, et al. Reduced treatment intensity in patients with early-stage Hodgkin's lymphoma. N Engl J Med 2010;363:640–52.
[3] Tubiana M, Henry-Amar M, Hayat M, Breur K, Werf-Messing B, Burgers M. Long-term results of the E.O.R.T.C. randomized study of irradiation and vinblastine in clinical stages I and II of Hodgkin's disease. Eur J Cancer 1979;15:645–57.
[4] Engert A, Schiller P, Josting A, et al. Involved-field radiotherapy is equally effective and less toxic compared with extended-field radiotherapy after four cycles of chemotherapy in patients with early-stage unfavorable Hodgkin's lymphoma: results of the HD8 trial of the German Hodgkin's Lymphoma Study Group. J Clin Oncol 2003;21:3601–8.
[5] Ferme C, Eghbali H, Meerwaldt JH, et al. Chemotherapy plus involved-field radiation in early-stage Hodgkin's disease. N Engl J Med 2007;357:1916–27.
[6] Maraldo MV, Aznar MC, Vogelius IR, Petersen PM, Specht L. Involved node radiation therapy: an effective alternative in early-stage Hodgkin lymphoma. Int J Radiat Oncol Biol Phys 2013;85:1057–65.
[7] Aleman BM, van den Belt-Dusebout AW, De Bruin ML, et al. Late cardiotoxicity after treatment for Hodgkin lymphoma. Blood 2007;109:1878–86.
[8] Ng AK, Bernardo MV, Weller E, et al. Second malignancy after Hodgkin disease treated with radiation therapy with or without chemotherapy: long-term risks and risk factors. Blood 2002;100:1989–96.
[9] De Bruin ML, Sparidans J, van't Veer MB, et al. Breast cancer risk in female survivors of Hodgkin's lymphoma: lower risk after smaller radiation volumes. J Clin Oncol 2009;27:4239–46.
[10] Hancock SL, Tucker MA, Hoppe RT. Factors affecting late mortality from heart disease after treatment of Hodgkin's disease. JAMA 1993;270:1949–55.
[11] Feng M, Moran JM, Koelling T, et al. Development and validation of a heart atlas to study cardiac exposure to radiation following treatment for breast cancer. Int J Radiat Oncol Biol Phys 2011;79:10–8.
[12] Jorgensen AYS, Maraldo MV, Brodin NP, et al. The effect on esophagus after different radiotherapy techniques for early stage Hodgkin's lymphoma. Acta Oncol 2013;52:1559–65.
[13] Maraldo MV, Brodin NP, Aznar MC, et al. Estimated risk of cardiovascular disease and secondary cancers with modern highly conformal radiotherapy for early-stage mediastinal Hodgkin lymphoma. Ann Oncol 2013;24:2113–8.
[14] Maraldo MV, Brodin P, Aznar MC, et al. Doses to carotid arteries after modern radiation therapy for Hodgkin lymphoma: is stroke still a late effect of treatment? Int J Radiat Oncol Biol Phys 2013;87:297–303.
[15] Maraldo MV, Brodin NP, Aznar MC, et al. Doses to head and neck normal tissues for early stage Hodgkin lymphoma after involved node radiotherapy. Radiother Oncol 2014;110:441–7.
[16] Carbone PP, Kaplan HS, Musshoff K, Smithers DW, Tubiana M. Report of the committee on Hodgkin's disease staging classification. Cancer Res 1971;31:1860–1.
[17] Eghbali H, Brice P, Creemers GJ, et al. Comparison of three radiation dose levels after EBVP regimen in favorable supradiaphragmatic clinical stages (CS) I–II Hodgkin's lymphoma (HL): preliminary results of the EORTC-GELA H9-F trial. Blood 2005;106:814.
[18] Ferme C, Divine M, Vranovsky A, et al. Four ABVD and involved-field radiotherapy in unfavorable supradiaphragmatic clinical stages (CS) I–II Hodgkin's lymphoma (HL): preliminary results of the EORTC-GELA H9-U trial. Blood 2005;106:813.
[19] Bufacchi A, Nardiello B, Capparella R, Begnozzi L. Clinical implications in the use of the PBC algorithm versus the AAA by comparison of different NTCP models/parameters. Radiat Oncol 2013;8:164.
[20] Deasy JO, Blanco AI, Clark VH. CERR: a computational environment for radiotherapy research. Med Phys 2003;30:979–85.
[21] Taylor CW, Nisbet A, McGale P, Darby SC. Cardiac exposures in breast cancer radiotherapy: 1950s–1990s. Int J Radiat Oncol Biol Phys 2007;69:1484–95.
[22] Taylor CW, Nisbet A, McGale P, et al. Cardiac doses from Swedish breast cancer radiotherapy since the 1950s. Radiother Oncol 2009;90:127–35.
[23] Travis LB, Gospodarowicz M, Curtis RE, et al. Lung cancer following chemotherapy and radiotherapy for Hodgkin's disease. J Natl Cancer Inst 2002;94:182–92.
[24] Travis LB, Hill DA, Dores GM, et al. Breast cancer following radiotherapy and chemotherapy among young women with Hodgkin disease. JAMA 2003;290:465–75.
[25] van Leeuwen FE, Klokman WJ, Stovall M, et al. Roles of radiation dose, chemotherapy, and hormonal factors in breast cancer following Hodgkin's disease. J Natl Cancer Inst 2003;95:971–80.
[26] Koh ES, Tran TH, Heydarian M, et al. A comparison of mantle versus involved-field radiotherapy for Hodgkin's lymphoma: reduction in normal tissue dose and second cancer risk. Radiat Oncol 2007;2:13.
[27] Ng A, Brock KK, Sharpe MB, Moseley JL, Craig T, Hodgson DC. Individualized 3D reconstruction of normal tissue dose for patients with long-term follow-up: a step toward understanding dose risk for late toxicity. Int J Radiat Oncol Biol Phys 2012;84:e557–63.
[28] Vordermark D, Seufert I, Schwab F, et al. 3-D reconstruction of anterior mantle-field techniques in Hodgkin's disease survivors: doses to cardiac structures. Radiat Oncol 2006;1:10.
[29] Specht L, Yahalom J, Illidge T, et al. Modern radiation therapy for Hodgkin lymphoma: field and dose guidelines from the International Lymphoma Radiation Oncology Group (ILROG). Int J Radiat Oncol Biol Phys 2014;89:854–62.